

# Equation of state of polydisperse hard-disk mixtures in the high-density regime

Andrés Santos,<sup>\*</sup> Santos B. Yuste,<sup>†</sup> and Mariano López de Haro<sup>‡</sup>  
*Departamento de Física and Instituto de Computación Científica Avanzada (ICCAEx),  
 Universidad de Extremadura, E-06006 Badajoz, Spain*

Vitaliy Ogarko<sup>§</sup>  
*Centre for Exploration Targeting, The University of Western Australia, Crawley WA 6009, Australia*  
 (Dated: March 16, 2017)

A proposal to link the equation of state of a monocomponent hard-disk fluid to the equation of state of a polydisperse hard-disk mixture is presented. Event-driven molecular dynamics simulations, performed to obtain data for the compressibility factor of the monocomponent fluid and of polydisperse mixtures with different size distributions, are used to assess the proposal and to infer the values of the compressibility factor of the monocomponent hard-disk fluid in the metastable region from those of mixtures in the high-density region. The collapse of the curves for the different mixtures is excellent in the stable region. In the metastable regime, except for two cases in which the ratio between the diameters of the biggest and the smallest disk is less than or equal to 1.2 and crystallization is present, the outcome of the approach exhibits a rather good performance.

## I. INTRODUCTION

The popularity in statistical physics of hard-core (hard-rod, hard-disk, hard-sphere, and hard-hypersphere) models for monocomponent fluids is undeniable. This is mostly due to the relative simplicity of their intermolecular interaction potentials. These models have also been important in the development of numerical simulation methods such as the Metropolis Monte Carlo algorithm [1] and the molecular dynamics (MD) method [2], which were first used in connection with monodisperse hard disks and monodisperse hard spheres in a box, respectively. Nevertheless and despite this simplicity, except for the hard-rod case, no exact analytical expressions for the corresponding free energies of these systems are available. Therefore, most of their qualitative features, such as the existence of a stable fluid branch, a (freezing) fluid-solid phase transition at a given packing fraction  $\phi_f$ , a region of fluid-solid coexistence, and a stable solid (crystalline) branch, have been determined mostly from computer simulations. It is usual to present the equilibrium phase diagram for such fluids as a graph in the thermodynamic planes pressure  $p$  vs density  $\rho$  or compressibility factor  $Z \equiv \beta p / \rho$  (where  $\beta \equiv 1/k_B T$ , with  $k_B$  the Boltzmann constant and  $T$  the absolute temperature) vs packing fraction  $\phi \equiv v_d \rho \sigma^d$  [ $\sigma$  being the diameter of the  $d$ -dimensional spheres,  $d$  the dimensionality, and  $v_d \equiv (\pi/4)^{d/2} \Gamma(1 + d/2)$ ]. Note that  $T$  only enters in the description as a scaling parameter and so these systems are often referred to as athermal.

The case of the hard-disk (HD) system is specially interesting since it also presents an hexatic phase characterized by short-ranged positional order, but quasi-long-ranged orientational order. Further, for this two-dimensional hard-core system the nature of the freezing and melting transitions (first reported in the pioneering work of Alder and Wainwright [3] and Alder, Hoover, and Wainwright [4]), the existence of a glass transition, and the location of the random close-packing fraction are still a source of debate. For deeper information on these issues, see Refs. 5–23.

On a different vein, polydispersity is known to be fundamental in studying important problems involving heterogeneous media, such as the mechanical properties of composite materials and the flow of fluids in porous media, and hence polydisperse systems also have received a lot of attention in the literature (see for instance Ref. 24 and references therein). Introducing polydispersity in size in hard-core models [in which case the packing fraction is  $\phi = v_d \rho M_d$  with  $M_n \equiv \int_0^\infty d\sigma \sigma^n f(\sigma)$  being the  $n$ th moment of the size distribution function  $f(\sigma)$ ] is known to lead to a rich phenomenology (not present in the monocomponent ones) that allows one for instance to avoid crystallization and modify the phase behavior [25–30] or to deal in principle with real polydisperse systems as diverse as colloidal suspensions, granular matter, plastics, foams, powders, monolayers of mixtures adsorbed on a substrate, nanoparticles, micelles, food emulsions, and cell tissues (see Ref. 31 and the literature cited therein). Particular interest in polydisperse HD systems has focused on packing problems, random sequential absorption, and glassy behavior. Although the list is by no means exhaustive, the interested reader may refer to Refs. 32–58 for more information on various aspects of these problems, whose discussion lies beyond the scope of the present paper.

Apart from the other characteristic regions in the phase diagram that have been mentioned above, one important feature that all the monocomponent hard-core

<sup>\*</sup> andres@unex.es; <http://www.unex.es/eweb/fisteor/andres/>

<sup>†</sup> santos@unex.es; <http://www.unex.es/eweb/fisteor/santos/>

<sup>‡</sup> malopez@unam.mx; <http://xml.cie.unam.mx/xml/tc/ft/mlh/>;  
 on sabbatical leave from Instituto de Energías Renovables, Universidad Nacional Autónoma de México (U.N.A.M.), Temixco, Morelos 62580, Mexico

<sup>§</sup> vitaliy.ogarko@uwa.edu.au

systems also present is that, beyond  $\phi_f$ , there is a region of metastable fluid states that overlaps the fluid-solid co-existence region and also partly the crystalline branch. Accessing this metastable fluid branch is difficult using simulations. In particular, computing the values of the thermodynamic variables with enough accuracy in the metastable states is quite a challenge so, in general, the metastable fluid branch remains as a largely unexplored ground. In previous work [59–66], we have provided different approximations for linking the equation of state (EoS) of a polydisperse hard-core mixture and the EoS of the monocomponent system. Our approach has, for instance and among other things, allowed us [63, 66] to infer the EoS of the hard-sphere fluid in the metastable fluid region from high-density simulation data of polydisperse hard-sphere mixtures. It also led us to estimate and put some order in a wealth of values for the random close-packing fraction of polydisperse hard-sphere mixtures from the knowledge of the random close-packing fraction of the monocomponent system [66].

The aim of this paper has several facets. On the one hand, given a polydisperse HD mixture with a certain size distribution at a packing fraction  $\phi$ , we will find an *effective* monocomponent HD fluid such that the free energy and the EoS of the former system can be mapped onto those of the latter. On the other hand, simulation data for the compressibility factor of a large number of polydisperse HD mixtures with different size distributions will also be presented. These data will then be used to assess the mapping “polydisperse mixture  $\leftrightarrow$  monocomponent fluid”. In particular, we will (a) check the collapse of all the mixture curves in a master one when plotted in the right variables and (b) use the high density data of the mixtures to infer the EoS of a HD fluid in the metastable region.

The paper is organized as follows. In Sec. II we present the development linking the free energy and EoS of a polydisperse HD mixture to those of the monocomponent system. Section III presents the simulation results of the compressibility factor of a variety of polydisperse HD mixtures with different size distributions and the assessment of the mapping “polydisperse mixture  $\leftrightarrow$  monocomponent fluid”, including the inference of the compressibility factor of the monocomponent HD fluid in the metastable region. The paper is closed in Sec. IV with further discussion and some concluding remarks.

## II. MAPPING BETWEEN THE EQUATION OF STATE OF THE POLYDISPERSE MIXTURE AND THAT OF THE MONOCOMPONENT SYSTEM FOR HARD DISKS

As mentioned above, an approach to link through an effective packing fraction  $\phi_{\text{eff}}$  the EoS of a monocomponent hard-sphere fluid to the EoS of a polydisperse hard-sphere mixture has been recently derived by application of some consistency conditions [64–66]. In this approach,

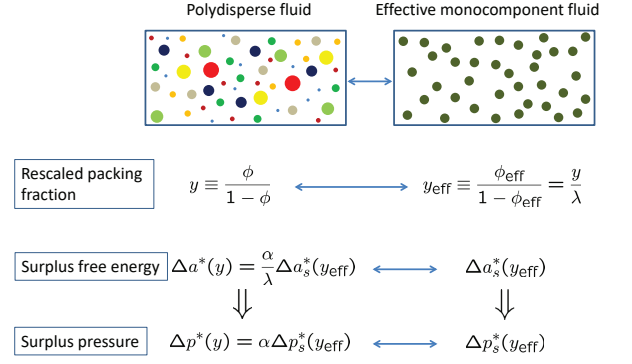


FIG. 1. Schematic view of the polydisperse  $\leftrightarrow$  monocomponent mapping represented by Eqs. (1)–(3).

the excess free energy per particle ( $a^{\text{ex}}$ ) of the mixture may be expressed in terms of the one of the monocomponent hard-sphere fluid ( $a_s^{\text{ex}}$ ) as

$$\beta a^{\text{ex}}(\phi) + \ln(1 - \phi) = \frac{\alpha}{\lambda} [\beta a_s^{\text{ex}}(\phi_{\text{eff}}) + \ln(1 - \phi_{\text{eff}})], \quad (1)$$

where the parameters  $\alpha$  and  $\lambda$  will be specified below, and the effective packing fraction  $\phi_{\text{eff}}$  of the monocomponent fluid is related to the packing fraction  $\phi$  of the polydisperse mixture through

$$\frac{\phi_{\text{eff}}}{1 - \phi_{\text{eff}}} = \frac{1}{\lambda} \frac{\phi}{1 - \phi}. \quad (2)$$

In turn, the mapping between the compressibility factor of the monocomponent system ( $Z_s$ ) and that of the polydisperse mixture ( $Z$ ) that is then obtained from Eq. (1) may be expressed as

$$\phi Z(\phi) - \frac{\phi}{1 - \phi} = \alpha \left[ \phi_{\text{eff}} Z_s(\phi_{\text{eff}}) - \frac{\phi_{\text{eff}}}{1 - \phi_{\text{eff}}} \right]. \quad (3)$$

In order to fix the parameters  $\alpha$  and  $\lambda$ , consistency of Eq. (3) to third order in density is imposed. This leads, in the three-dimensional case [66], to  $\lambda = m_3/m_2^2 \geq 1$  and  $\alpha = \lambda/m_2 \leq \lambda$ , where  $m_n \equiv M_n/M_1^n$  is the  $n$ th dimensionless moment.

An interesting consequence of Eq. (3) is that one can invert it to *infer* the monocomponent EoS from that of the polydisperse fluid. The degree of collapse of the mapping from different functions  $Z(\phi)$  onto a *common* function  $Z_s(\phi_{\text{eff}})$  is an efficient way of assessing Eq. (3) without having to use an externally imposed EoS.

Equations (1)–(3) lend themselves to an insightful physical interpretation [67]. First, note that the ratio  $y \equiv \phi/(1 - \phi)$  represents a *rescaled* packing fraction, i.e., the ratio between the volume occupied by the spheres and the remaining *void* volume. Thus, Eq. (2) dictates that the effective monocomponent fluid associated with a given mixture has a rescaled packing fraction  $y_{\text{eff}} \equiv \phi_{\text{eff}}/(1 - \phi_{\text{eff}})$  that is  $\lambda$  times smaller than that of

the mixture. Next,  $\Delta p^*(y) \equiv \phi Z(\phi) - \phi/(1 - \phi)$  represents a (reduced) “surplus” pressure with respect to the ideal-gas value *corrected* by the void volume. Analogously, we can define the “surplus” free energy per particle  $\Delta a^*(y) \equiv \beta a^{\text{ex}}(\phi) + \ln(1 - \phi)$  as the difference between the (reduced) free energy per particle and the ideal-gas value corrected by the void volume. In terms of those quantities, Eqs. (1) and (3) establish that the surplus free energy  $\Delta a^*$  and pressure  $\Delta p^*$  of the polydisperse fluid are just proportional to their respective monocomponent counterparts  $\Delta a_s^*$  and  $\Delta p_s^*$ . This is schematically depicted in Fig. 1. While the surplus free energy of the polydisperse fluid is never larger than that of the effective monocomponent fluid (since  $\alpha/\lambda \leq 1$ ), the surplus pressure  $\Delta p^*$  can be larger than, equal to, or smaller than  $\Delta p_s^*$  (since  $\alpha - 1$  has not a definite sign).

It should be stressed that the proposal implied by Eq. (3) may be interpreted in two directions. On the one hand, if  $Z_s$  is known as a function of  $\phi_{\text{eff}}$ , then one can readily compute  $Z$  as a function of  $\phi$ ,  $\phi_{\text{eff}}$  and  $\phi$  being of course related through Eq. (2). On the other hand, if  $Z(\phi)$  is known in a high enough density region, then the values of  $Z_s(\phi_{\text{eff}})$  may be inferred from those of the mixture even in regions where obtaining them from simulation is either difficult or not feasible, such as the metastable fluid branch.

Although initially derived for three-dimensional hard-sphere systems [65, 66], the physical interpretation of Eqs. (1)–(3) suggests their heuristic generalization to any dimensionality  $d \neq 3$ . In that case, the parameters  $\lambda$  and  $\alpha$  can be determined again by imposing consistency with the second and third virial coefficients [67]. This leads to

$$\lambda = \frac{\bar{B}_2 - 1}{b_2 - 1} \frac{b_3 - 2b_2 + 1}{\bar{B}_3 - 2\bar{B}_2 + 1}, \quad \alpha = \lambda^2 \frac{\bar{B}_2 - 1}{b_2 - 1}, \quad (4)$$

where  $\bar{B}_n \equiv B_n/(v_d M_d)^{n-1}$  and  $b_n \equiv B_n/(v_d M_d)^{n-1}$  are reduced virial coefficients of the mixture and the monocomponent fluid, respectively ( $B_n$  being the standard virial coefficients).

In what follows, we will particularize to the case of HD systems ( $d = 2$ ), in which case  $v_2 = \pi/4$ ,  $b_2 = 2$ ,  $b_3 = 4(4/3 - \sqrt{3}/\pi) \simeq 3.12802$  and the second virial coefficient of the polydisperse HD mixture is given exactly by

$$\bar{B}_2 = 1 + m_2^{-1}. \quad (5)$$

On the other hand, given a size distribution  $f(\sigma)$ , the *exact* third virial coefficient of a polydisperse mixture of *additive* HDs is a not expressible in terms of moments. Its explicit expression is [67]

$$B_3 = \frac{\pi}{2} \int_0^\infty d\sigma_1 f(\sigma_1) \int_0^\infty d\sigma_2 f(\sigma_2) \sigma_{12}^2 \times \int_0^\infty d\sigma_3 f(\sigma_3) \mathcal{A}_{\sigma_{13}, \sigma_{23}}(\sigma_{12}), \quad (6)$$

where  $\sigma_{ij} = \frac{1}{2}(\sigma_i + \sigma_j)$  and

$$\mathcal{A}_{a,b}(r) = a^2 \cos^{-1} \frac{r^2 + a^2 - b^2}{2ar} + b^2 \cos^{-1} \frac{r^2 + b^2 - a^2}{2br} - \frac{1}{2} \sqrt{2r^2(a^2 + b^2) - (b^2 - a^2)^2 - r^4} \quad (7)$$

is the intersection area of two circles of radii  $a$  and  $b$  whose centers are separated by a distance  $r$ .

Therefore, for HD fluids Eq. (3) becomes

$$\phi Z(\phi) - \frac{\phi}{1 - \phi} = \frac{\lambda^2}{m_2} \left[ \phi_{\text{eff}} Z_s(\phi_{\text{eff}}) - \frac{\phi_{\text{eff}}}{1 - \phi_{\text{eff}}} \right] \quad (8)$$

or, equivalently,

$$\Delta p^*(y) = \frac{\lambda^2}{m_2} \Delta p_s^*(y/\lambda), \quad (9)$$

with

$$\lambda = \frac{b_3 - 3}{(\bar{B}_3 - 1)m_2 - 2}. \quad (10)$$

It is worthwhile noting that in the Scaled Particle Theory (SPT) for HD systems [68–70] one simply has  $\Delta p_s^*(y) = y^2$  and  $\Delta p^*(y) = m_2^{-1} y^2$ , so that Eq. (9) is identically satisfied for *arbitrary* values of  $\lambda$ . In the more general case, however, the polydisperse  $\leftrightarrow$  monocomponent mapping depends on  $\lambda$ , as given by Eq. (10), to guarantee that the third virial coefficient of the mixture is exactly retained. On the other hand, this latter requirement implies an added difficulty since, as said before, the exact determination of  $\bar{B}_3$  via Eq. (6) cannot be carried out from the knowledge of just the first few moments of the size distribution  $f(\sigma)$ . Therefore, it seems practical to replace the exact formula (6) by an approximate simpler one. In Ref. [71] three of us proposed an approximate expression of  $B_3$  for nonadditive  $d$ -dimensional hard-sphere mixtures. Its particularization to additive HD mixtures yields [67]

$$\bar{B}_3^{\text{app}} = 1 + \frac{b_3 - 1}{m_2}. \quad (11)$$

Using this approximation in Eq. (10) we obtain  $\lambda = 1$  and  $\alpha = m_2^{-1}$ . Thus,  $\phi_{\text{eff}} = \phi$  and Eq. (8) becomes

$$Z(\phi) - \frac{1}{1 - \phi} = \frac{1}{m_2} \left[ Z_s(\phi) - \frac{1}{1 - \phi} \right]. \quad (12)$$

Interestingly enough, this mapping coincides with an approximate relationship between both compressibility factors that has been proposed earlier and derived from different methods [59, 62].

Equation (8), together with Eqs. (2), (6), (7), and (10), on the one hand, and Eq. (12), on the other hand, provide two different (approximate) connections between the compressibility factor of polydisperse HD mixtures of

given size distribution and that of the monocomponent HD fluid.

For later comparison, we also include here another theoretical mapping proposed by Barrio and Solana [72–74] which reads

$$Z(\phi) - 1 = \left[ \frac{1 + m_2^{-1}}{2} - \left( b_3 \frac{1 + m_2^{-1}}{4} - \frac{\bar{B}_3}{2} \right) \phi \right] \times [Z_s(\phi) - 1]. \quad (13)$$

Again the mapping in Eq. (13) is consistent with  $\bar{B}_2$  and  $\bar{B}_3$  but cannot be expressed in terms of moments unless  $\bar{B}_3$  is replaced by  $\bar{B}_3^{\text{app}}$ .

The three above proposals for the mapping between  $Z$  and  $Z_s$  will be assessed in Sec. III.

### III. RESULTS

#### A. Systems examined

In order to test the usefulness of the approximations implied by Eqs. (8), (12), and (13), the following classes of size distributions have been chosen. First, binary (B) mixtures having a discrete composition characterized by

$$f(\sigma) = (1 - x)\delta(\sigma - a) + x\delta(\sigma - aw), \quad (14)$$

where  $a$  and  $w$  are the small diameter and the ratio of the big to the small diameter, respectively, and  $x$  is the mole fraction of the big species. The associated  $n$ th-order moment is  $M_n = a^n(1 - x + xw^n)$ . Next, the top-hat (TH) distribution

$$f(\sigma) = \frac{1}{a(w - 1)}\Theta(\sigma - a)\Theta(aw - \sigma), \quad (15)$$

where  $\Theta(x)$  is the Heaviside step function. In this case,  $M_n = a^n(w^{n+1} - 1)/(w - 1)(n + 1)$ . Finally, we consider

$$f(\sigma) = \frac{aw\sigma^{-2}}{w - 1}\Theta(\sigma - a)\Theta(aw - \sigma), \quad (16)$$

so that the distribution decays in the interval  $a < \sigma < aw$  as an inverse power (IP) law of second order. Here,  $M_1 = aw(\ln w)/(w - 1)$  and  $M_n = a^n(w^n - w)/(w - 1)(n - 1)$  for  $n \neq 1$ .

Table I contains a list of the 26 mixtures (B1–B8, TH1–TH11, IP1–IP7) examined in this paper, together with the corresponding values of their exact second and third virial coefficients, as given by Eqs. (5) and (6), respectively. Note that, except in the binary cases, the values of  $\bar{B}_3$  need to be obtained numerically. Table I also includes the values of  $\lambda$ , as obtained from Eq. (10), and of  $\alpha = \lambda^2/m_2$ , as well as those of the approximate third virial coefficient, Eq. (11).

A convenient measure of the “degree of dispersity” in a mixture can be taken as the reduced variance  $m_2 - 1$  of the size distribution. Equivalently, according to Eq. (5), the degree of dispersity can be measured

by  $2 - \bar{B}_2 = 1 - m_2^{-1}$ . In a B mixture at a fixed value of  $w$ ,  $m_2$  takes a maximum value  $m_2 = (1 + w)^2/4w$  at  $x = 1/(1 + w)$ ; this maximum value monotonically increases (almost linearly) without upper bound as  $w$  increases. In the case of IP mixtures, one has  $m_2 = (w - 1)^2/w(\ln w)^2$ , which again grows unbounded (but much more slowly) with increasing  $w$ . On the other hand,  $m_2 = 4(1 + w + w^2)/3(1 + w)^2$  for TH mixtures, this quantity being now upper bounded by  $m_2 = \frac{4}{3}$ . Taking all of this into account, we can order the 26 mixtures of Table I in ascending degree of dispersity as TH1, TH2, TH3, IP1, IP2, B1, IP3, TH4, IP4, IP5, TH5, IP6, B2, TH6, IP7, TH7, TH8, TH9, TH10, TH11, B3, B4, B5, B6, B7, and B8. Interestingly, even though  $\bar{B}_3$  is not expressible in terms of moments, it turns out that the same ordering is obtained if the degree of dispersity is measured by  $b_3 - \bar{B}_3$ . The same happens if the dispersity criterion is  $\lambda - 1$ , except for the permutation B2 $\leftrightarrow$ TH6 and IP7 $\leftrightarrow$ TH7.

It can be observed from Table I that  $\bar{B}_3^{\text{app}}$  tends to overestimate  $\bar{B}_3$  but otherwise it is always a very good approximation, with a maximum relative deviation of 1.07% (mixture B5). Analogously,  $\lambda \leq 1.11$ , except in the mixtures B3–B8, where  $\lambda$  increases rather rapidly with dispersity. It seems paradoxical that  $\lambda$  can be as large as  $\lambda = 2.82$  (mixture B8) even though  $\delta\bar{B}_3 \equiv \bar{B}_3^{\text{app}} - \bar{B}_3$  is relatively small (for instance,  $\delta\bar{B}_3 = 0.008$  in the case of B8). In order to understand this, note that Eq. (10) can be recast as  $\lambda^{-1} = 1 - \delta\bar{B}_3/(b_3 - 3)(\bar{B}_2 - 1)$ . As long as  $\delta\bar{B}_3/(b_3 - 3) \ll \bar{B}_2 - 1$ , as happens typically if  $\bar{B}_2 > 1.7$ ,  $\lambda$  is only slightly larger than 1. On the other hand, as dispersity increases,  $\bar{B}_2$  becomes closer to 1 and, therefore,  $\lambda$  visibly departs from 1.

#### B. Molecular dynamics simulations

We have used event-driven MD simulations with a modification of the Lubachevsky–Stillinger algorithm [75–77] to compute the compressibility factors of poly-disperse HD mixtures having the 26 size distributions described by Table I, as well as for the monocomponent HD system. In each case, a single MD run was employed to span a wide range of packing fractions (from  $\phi \approx 0$  to  $\phi \approx 0.85$ ) by expanding the area of the disks. More specifically, in our simulations the diameter  $\sigma_i(t)$  of particle  $i$  was grown according to the linear law  $\dot{\sigma}_i(t) = \Gamma\sqrt{E/M}\sigma_i(t)/\sigma_{\text{max}}(t)$ , where  $E$  and  $M$  are the total energy and mass, respectively,  $\sigma_{\text{max}}(t)$  is the largest diameter in the system, and the ratio  $\sigma_i(t)/\sigma_{\text{max}}(t)$  is independent of time. We used slow growth rates  $\Gamma = 1.6 \times 10^{-4}$  to  $1.6 \times 10^{-5}$ , a number of particles  $N = 2^{12} = 4096$  to  $2^{14} = 16,384$ , and periodic boundary conditions.



TABLE I. Values of  $\bar{B}_2$ ,  $\bar{B}_3$ ,  $\bar{B}_3^{\text{app}}$ ,  $\lambda$ , and  $\alpha$  for the different polydisperse HD mixtures examined in this work.

Label	$x$	$w$	$\bar{B}_2$	$\bar{B}_3$	$\bar{B}_3^{\text{app}}$	$\lambda$	$\alpha$
B1	0.5	1.4	1.97297	3.06851	3.07050	1.01630	1.00495
B2	0.3	2	1.88947	2.88496	2.89282	1.07412	1.02621
B3	0.25	4	1.64474	2.35456	2.37201	1.26816	1.03689
B4	0.14	6	1.48983	2.02135	2.04237	1.50420	1.10830
B5	0.07	14	1.24902	1.51371	1.52991	2.03367	1.02989
B6	0.04	22	1.16661	1.34172	1.35456	2.51284	1.05206
B7	0.03	30	1.12502	1.25584	1.26605	2.76326	0.95463
B8	0.025	40	1.09520	1.19471	1.20258	2.82185	0.75802
TH1		1.1	1.99924	3.12635	3.12641	1.00046	1.00016
TH2		1.2	1.99725	3.12196	3.12217	1.00166	1.00056
TH3		1.4	1.99083	3.10780	3.10849	1.00553	1.00181
TH4		2	1.96429	3.04943	3.05202	1.02136	1.00593
TH5		3	1.92308	2.95922	2.96432	1.04515	1.00831
TH6		5	1.87097	2.84588	2.85343	1.07264	1.00210
TH7		10	1.81757	2.73069	2.73980	1.09530	0.98083
TH8		20	1.78563	2.66232	2.67183	1.10447	0.95835
TH9		30	1.77417	2.63789	2.64744	1.10663	0.94808
TH10		100	1.75743	2.60233	2.61181	1.10845	0.93062
TH11		500	1.75150	2.58977	2.59920	1.10865	0.92367
IP1		1.4	1.99062	3.10734	3.10805	1.00570	1.00195
IP2		1.6	1.98179	3.08789	3.08927	1.01114	1.00378
IP3		1.8	1.97170	3.06566	3.06779	1.01744	1.00588
IP4		2	1.96091	3.04191	3.04483	1.02428	1.00813
IP5		2.4	1.93850	2.99266	2.99715	1.03883	1.01280
IP6		3	1.90521	2.91960	2.92631	1.06138	1.01975
IP7		4	1.85414	2.80783	2.81762	1.09835	1.03041

### C. Assessment of the mapping

Figure 2(a) shows all the functions  $Z(\phi)$  for those 26 mixtures and for the monocomponent system. As expected, each mixture differs in the values of  $Z$  for a common  $\phi$ . If the mapping “polydisperse mixture  $\leftrightarrow$  monocomponent fluid” as given by Eq. (8) works, a high degree of collapse of all the curves should be expected when the inferred monocomponent quantity  $Z_s(\phi_{\text{eff}})$  is plotted instead of  $Z(\phi)$ . This is shown in Fig. 2(b), where an excellent collapse of all the mixture curves is observed in the stable region ( $\phi_{\text{eff}} \lesssim 0.7$ ), the collapse keeping being rather good (although, of course, not perfect) in the metastable region ( $\phi_{\text{eff}} > 0.7$ ), except for the mixtures TH1 and TH2, in which the ratio between the diameters of the biggest and the smallest disk is less than or equal to  $w = 1.2$ . Those latter curves exhibit crystallization effects in that region and thus follow trends similar to that of the monocomponent fluid. This observation agrees with the result of Speedy [7], who also pointed out that, in the case of equimolar binary HD mixtures, freezing to a mixed crystal occurs when  $w < 1.2$  while they may reach the metastable fluid region when  $w \geq 1.3$ . On the other hand, a higher degree of dispersity (say  $m_2 \gtrsim 1.01$ ) allows one to frustrate equilibration to a crystal phase and explore the metastable fluid branch, which is practically inaccessible for the monocomponent fluid. Interestingly, we have checked (not shown) that the extrapolations in the metastable domain of known accurate EoS for the

monocomponent HD fluid [78–82] agree fairly well with the inferred values of  $Z_s$  in that domain.

Figure 3 shows the inferred  $Z_s(\phi)$  as obtained with the simplified mapping given by Eq. (12), i.e., with  $\lambda \rightarrow 1$  or  $B_3 \rightarrow \bar{B}_3^{\text{app}}$ . Despite this simplification, we get a collapse of the mixture curves practically as good as the one shown in Fig. 2(b), although the mapping corresponding to Eq. (8) is somewhat more accurate in the metastable region. Notwithstanding this, it should be pointed out that the mapping (8) has two drawbacks with respect to the mapping (12). First, it requires the numerical evaluation of the scaling parameter  $\lambda$  via Eqs. (6) and (10). Second, since  $\phi_{\text{eff}} < \phi$ , one has to go to higher packing fractions of the mixture to get access to the high-density region of the monocomponent system. This is a drawback because the simulation results for the polydisperse mixtures become noisier, and hence more unreliable, as the packing fraction of the mixture increases, due to diverging collision rates. The previous feature is illustrated in Fig. 4, where we have joined with straight lines the points connecting the packing fraction  $\phi$  of the mixture B8 with the corresponding effective value  $\phi_{\text{eff}}$  of the monocomponent fluid. Thus, according to Eq. (8), the values of  $Z$  for the mixture B8 on the region  $0 < \phi < 0.87$  map onto values of  $Z_s$  in the narrower region  $0 < \phi_{\text{eff}} < 0.70$ . In contrast, Eq. (12) allows one to infer  $Z_s$  at the same packing fractions as for the mixture.

As said at the end of Sec. II, a mapping alternative to Eqs. (8) and (12) is represented by Eq. (13). The asso-

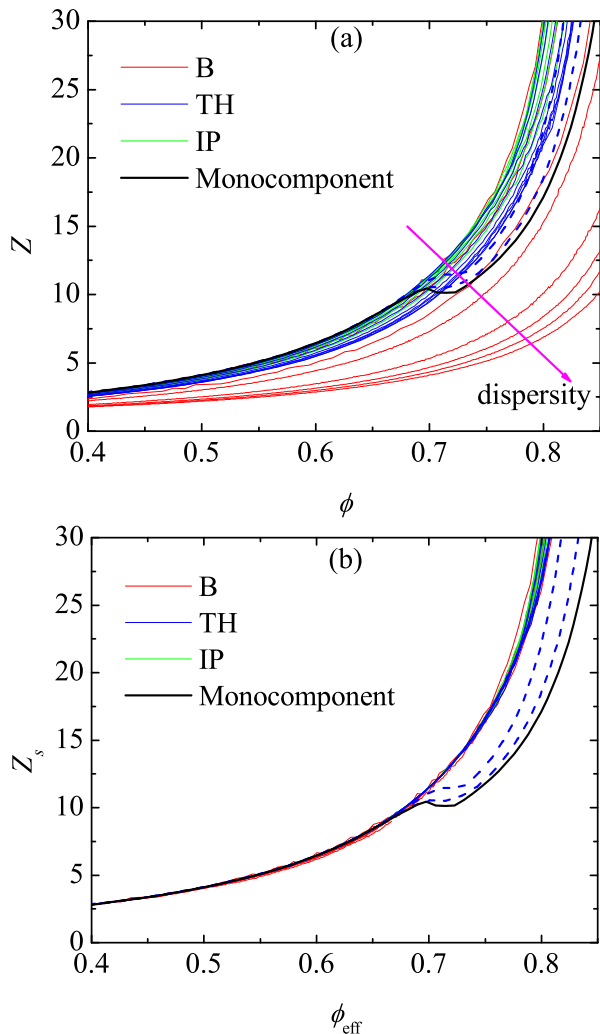


FIG. 2. (a) Plot of  $Z(\phi)$  as obtained from our simulations for the monocomponent HD fluid and for various polydisperse HD mixtures. (b) Plot of the inferred monocomponent compressibility factor  $Z_s(\phi_{\text{eff}})$  as obtained from Eqs. (2) and (8), complemented by Eqs. (6) and (10). The thick black solid line corresponds to the monocomponent system, while the thin red (B1–B8), blue (TH3–TH11), and green (IP1–IP7) solid lines correspond to polydisperse systems. The two thick blue dashed lines refer to mixtures TH1 and TH2.

ciated inferred  $Z_s(\phi)$  is shown in Fig. 5. Here, the true values of  $\bar{B}_3$  have been used, but we have checked that the curves are practically indistinguishable from those obtained if  $\bar{B}_3$  is replaced by  $\bar{B}_3^{\text{app}}$  as given in Eq. (11). While the mapping (13) does a good job for not too disparate mixtures (say  $m_2 < 2$  or, equivalently,  $\bar{B}_2 > 1.5$ ), it clearly fails for the mixtures B4–B8, even in the stable region. In fact, Eq. (13) is inconsistent with the exact limit of a binary mixture in which the small disks are point particles [83].

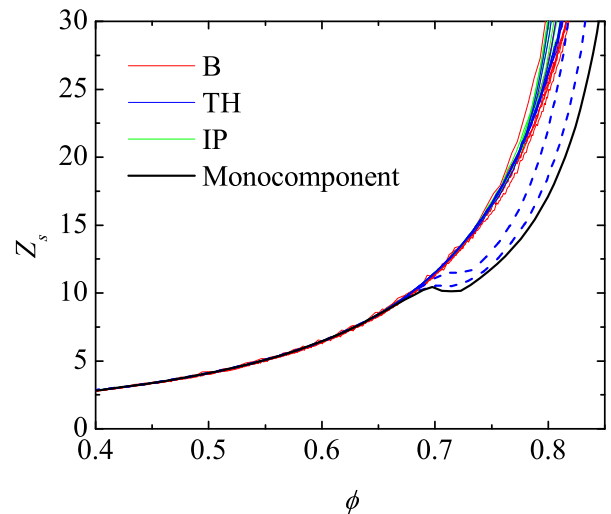


FIG. 3. Plot of the inferred monocomponent compressibility factor  $Z_s(\phi)$  as obtained from Eq. (12). The meaning of the curves is the same as in Fig. 2.

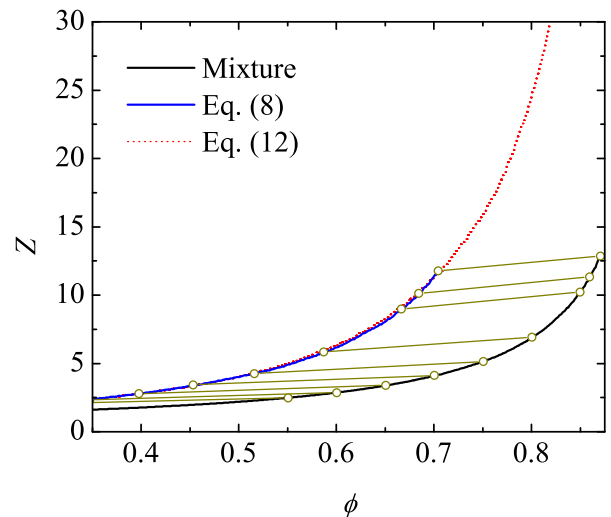


FIG. 4. Plot of the compressibility factor for the mixture B8 (black solid line) and for the inferred monocomponent compressibility factor as obtained from Eq. (8) (blue solid line) and from Eq. (12) (dotted red line). The circles joined by straight lines denote pairs  $(\phi_{\text{eff}}, \phi)$  as given by Eq. (2).

#### IV. CONCLUDING REMARKS

In this paper we have presented a heuristic ansatz for the relationship between the excess Helmholtz free energy of a polydisperse HD mixture,  $a^{\text{ex}}$ , and the one of the monocomponent HD fluid,  $a_s^{\text{ex}}$ . Such an ansatz maintains the form introduced earlier for the three-dimensional case [66] and allowed us to derive a link between both compressibility factors in which  $Z$  and  $Z_s$  are evaluated at *different* packing fractions.

The mapping may be used in the two directions: from a known compressibility factor  $Z_s$  as a function of the

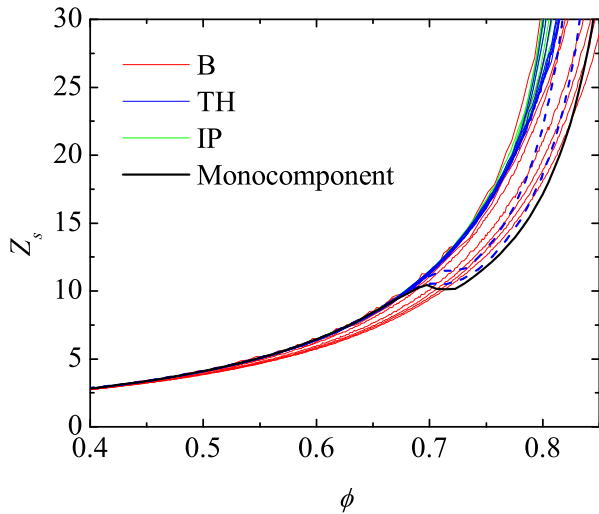


FIG. 5. Plot of the inferred monocomponent compressibility factor  $Z_s(\phi)$  as obtained from Eq. (13) with  $\bar{B}_3$  given by Eq. (6). The meaning of the curves is the same as in Fig. 2.

packing fraction  $\phi_{\text{eff}}$  one may obtain the compressibility factor of *any* polydisperse mixture at the corresponding packing fraction  $\phi$ ; on the other hand, from values of  $Z(\phi)$  at a high enough density one may compute the corresponding values of  $Z_s(\phi_{\text{eff}})$  in difficult or inaccessible density regions from the simulation point of view. The only information required in the mapping are the second and third virial coefficients of the polydisperse mixture and those of the monocomponent system. Thus, the main asset of our approach is its relative simplicity.

In the two-dimensional case examined here, where the monocomponent virial coefficients are exactly known, the expressions of the required virial coefficients of the mixture for a given size distribution were explicitly provided. It turns out that, as it happened in three dimensions, the second virial coefficient is a rather simple function of the first two moments of the size distribution. On the other hand, in contrast with what happened in the case of hard spheres, the third virial coefficient for a polydisperse HD mixture may not be expressed in terms of the moments of the size distribution, but is nevertheless amenable to explicit evaluation. If one makes a further approximation, namely the replacement of the exact third virial coefficient by the approximate value  $\bar{B}_3^{\text{app}}$  (also given in terms of the first two moments), one gets another mapping which coincides with one derived earlier with a dif-

ferent method in which both compressibility factors are evaluated at the same packing fraction [59, 62]. With these two proposals, and making use of the compressibility factors obtained from MD simulations for a variety of polydisperse HD mixtures that cover a wide density range, we have been able to derive the values of the compressibility factor of a monocomponent HD fluid in the metastable fluid branch beyond the fluid-solid phase transition.

While the collapse of the curves corresponding to the very different mixtures is not perfect, it is quite reasonable both in the stable and metastable regions and allows one to identify systems in which some degree of crystallization may still be present. This outcome points out to the usefulness of our approach to infer the EoS of the monocomponent HD from the knowledge of the high-density data of polydisperse HD mixtures, thus circumventing the problem of entering into the metastable fluid branch that is present in simulations. It turns out that with the mapping based on  $\bar{B}_3^{\text{app}}$  the inferred EoS of the monocomponent system is almost as accurate as the one without such an approximation and superior to the (also simple) proposal of Barrio and Solana [72–74], especially in the case of very disparate mixtures. Therefore this seems to be a reasonable compromise between accuracy and simplicity.

Finally, as done in the case of hard spheres in Ref. [66], it would be tempting to try to estimate the jamming packing fraction  $\phi_J$  of a given mixture from the knowledge of the random close-packing fraction  $\phi_{\text{rcp}}$  of the monocomponent system. In fact, the reasonably good degree of collapse observed in Fig. 2(b) for very high packing fractions provides some support to the use of Eq. (2) for such an estimate. Hence, in this case  $\phi_J \approx \lambda/(\lambda + \phi_{\text{rcp}}^{-1} - 1)$  with  $\lambda$  given by Eqs. (6), (7), and (10).

## ACKNOWLEDGMENTS

We want to thank Adrián Huerta for a fruitful exchange of correspondence. A.S., S.B.Y., and M.L.H. acknowledge the financial support of the Ministerio de Economía y Competitividad (Spain) through Grant No. FIS2016-76359-P and the Junta de Extremadura (Spain) through Grant No. GR15104, both partially financed by FEDER funds. M.L.H. also acknowledges CONACYT for a sabbatical grant.

---

[1] N. Metropolis, A. W. Rosenbluth, M. N. Rosenbluth, A. H. Teller, and E. Teller, J. Chem. Phys. **21**, 1087 (1953).  
 [2] B. J. Alder and T. E. Wainwright, J. Chem. Phys. **27**, 1208 (1957).  
 [3] B. J. Alder and T. E. Wainwright, Phys. Rev. **127**, 359

(1962).  
 [4] B. J. Alder, W. G. Hoover, and T. E. Wainwright, Phys. Rev. Lett. **11**, 241 (1963).  
 [5] J. G. Berryman, Phys. Rev. A **27**, 1053 (1983).  
 [6] R. J. Speedy and H. Reiss, Mol. Phys. **72**, 1015 (1991).  
 [7] R. J. Speedy, J. Chem. Phys. **110**, 4559 (1999).

- [8] L. Santen and W. Krauth, “Liquid, glass and crystal in two-dimensional hard disks,” arXiv:cond-mat/0107459 (2001).
- [9] O. Uche, F. Stillinger, and S. Torquato, *Physica A* **342**, 428 (2004).
- [10] N. Xu, J. Blawdziewicz, and C. S. O’Hern, *Phys. Rev. E* **71**, 061306 (2005).
- [11] C. H. Mak, *Phys. Rev. E* **73**, 065104 (2006).
- [12] A. Huerta, D. Henderson, and A. Trokhymchuk, *Phys. Rev. E* **74**, 061106 (2006).
- [13] A. Donev, F. H. Stillinger, and S. Torquato, *Phys. Rev. Lett.* **96**, 225502 (2006).
- [14] A. Donev, F. H. Stillinger, and S. Torquato, *J. Chem. Phys.* **127**, 124509 (2007).
- [15] J. J. Kozak, J. Brzezinski, and S. A. Rice, *J. Phys. Chem. B* **112**, 16059 (2008).
- [16] J. Zhang, T. S. Majmudar, M. Sperl, and R. P. Behringer, *Soft Matter* **6**, 2982 (2010).
- [17] J. Piasecki, P. Szymczak, and J. J. Kozak, *J. Chem. Phys.* **133**, 164507 (2010).
- [18] G. Parisi and F. Zamponi, *Rev. Mod. Phys.* **82**, 789 (2010).
- [19] S. Torquato and F. H. Stillinger, *Rev. Mod. Phys.* **82**, 2633 (2010).
- [20] E. P. Bernard and W. Krauth, *Phys. Rev. Lett.* **107**, 155704 (2011).
- [21] X. Xu and S. A. Rice, *Phys. Rev. E* **83**, 021120 (2011).
- [22] A. Huerta, V. Carrasco-Fadanelli, and A. Trokhymchuk, *Condens. Matter Phys.* **15**, 43604 (2012).
- [23] R. Sánchez, I. C. Romero-Sánchez, S. Santos-Toledano, and A. Huerta, *Rev. Mex. Fís.* **60**, 136 (2014).
- [24] P. A. Rijkvold and G. Stell, *Chem. Eng. Comm.* **51**, 233 (1987).
- [25] E. Dickinson, *Chem. Phys. Lett.* **57**, 148 (1978).
- [26] E. Dickinson, *J. Chem. Soc. Faraday Trans. 2* **76**, 1458 (1980).
- [27] E. Dickinson, *Chem. Phys. Lett.* **79**, 578 (1981).
- [28] R. Blaak, *J. Chem. Phys.* **112**, 9041 (2000).
- [29] S. Pronk and D. Frenkel, *Phys. Rev. E* **69**, 066123 (2004).
- [30] K. V. Tretyakov and K. W. Wojciechowski, *J. Chem. Phys.* **136**, 204506 (2012).
- [31] T. S. Ingebrigtsen and H. Tanaka, *J. Phys. Chem. B* **119**, 11052 (2015).
- [32] E. L. Hinrichsen, J. Feder, and T. Jossang, *J. Stat. Phys.* **44**, 793 (1986).
- [33] D. Bideau, A. Gervois, L. Oger, and J. P. Troadec, *J. Phys. France* **47**, 1697 (1986).
- [34] G. C. Barker and M. J. Grimson, *J. Phys.: Condens. Matter* **1**, 2779 (1989).
- [35] J. Talbot and P. Schaaf, *Phys. Rev. A* **40**, 422 (1989).
- [36] G. Tarjus and J. Talbot, *J. Phys. A: Math. Gen.* **24**, L913 (1991).
- [37] P. Meakin and R. Jullien, *Phys. Rev. A* **46**, 2029 (1992).
- [38] Z. Adamczyk, B. Siwek, M. Zembala, and P. Weroniski, *J. Co* **185**, 236 (1997).
- [39] J. J. Gray, D. H. Klein, B. A. Korgel, and R. T. Bonnecaze, *Langmuir* **17**, 2317 (2001).
- [40] J. J. Gray and R. T. Bonnecaze, *Langmuir* **17**, 7935 (2001).
- [41] T. Okubo and T. Odagaki, *J. Phys.: Condens. Matter* **16**, 6651 (2004).
- [42] G. Tarjus, S. A. Kivelson, Z. Nussinov, and P. Viot, *J. Phys.: Condens. Matter* **17**, R1143 (2005).
- [43] A. Chremos and P. J. Camp, *Phys. Rev. E* **76**, 056108 (2007).
- [44] T. S. Majmudar, M. Sperl, S. Luding, and R. P. Behringer, *Phys. Rev. Lett.* **98**, 058001 (2007).
- [45] M. Clusel, E. I. Corwin, A. O. N. Siemens, and J. Brujic, *Nature* **460**, 611 (2009).
- [46] F. Weysser and D. Hajnal, *Phys. Rev. E* **83**, 041503 (2011).
- [47] T. Kawasaki and H. Tanaka, *J. Phys.: Condens. Matter* **23**, 194121 (2011).
- [48] L. J. Bonales, F. Martínez-Pedrero, M. A. Rubio, R. G. Rubio, and F. Ortega, *Langmuir* **28**, 16555 (2012).
- [49] M. P. Miklius and S. Hilgenfeldt, *Phys. Rev. Lett.* **108**, 015502 (2012).
- [50] S. Hilgenfeldt, *Philos. Mag.* **93**, 4018 (2013).
- [51] D. Asenjo, F. Paillusson, and D. Frenkel, *Phys. Rev. Lett.* **112**, 098002 (2014).
- [52] Y. Jiao, T. Lau, H. Hatzikirou, M. Meyer-Hermann, J. C. Corbo, and S. Torquato, *Phys. Rev. E* **89**, 022721 (2014).
- [53] J. S. Langer, *Rep. Prog. Phys.* **77**, 042501 (2014).
- [54] J. T. Kindt, *J. Chem. Phys.* **143**, 124109 (2015).
- [55] S. Martiniani, K. J. Schrenk, J. D. Stevenson, D. J. Wales, and D. Frenkel, *Phys. Rev. E* **93**, 012906 (2016).
- [56] Y. Zhou and S. T. Milner, *Soft Matter* **12**, 7281 (2016).
- [57] M. Isobe, *Mol. Simul.* **42**, 1317 (2016).
- [58] M. Isobe, A. S. Keys, D. Chandler, and J. P. Garrahan, *Phys. Rev. Lett.* **117**, 145701 (2016).
- [59] A. Santos, S. B. Yuste, and M. López de Haro, *Mol. Phys.* **96**, 1 (1999).
- [60] A. Santos, *Mol. Phys.* **96**, 1185 (1999), Erratum: **99**, 617 (2001).
- [61] M. López de Haro, S. B. Yuste, and A. Santos, *Mol. Phys.* **104**, 3461 (2006).
- [62] M. López de Haro, S. B. Yuste, and A. Santos, in *Theory and Simulation of Hard-Sphere Fluids and Related Systems*, Lecture Notes in Physics, Vol. 753, edited by A. Mulero (Springer-Verlag, Berlin, 2008) pp. 183–245.
- [63] A. Santos, S. B. Yuste, and M. López de Haro, *J. Chem. Phys.* **135**, 181102 (2011).
- [64] A. Santos, *J. Chem. Phys.* **136**, 136102 (2012).
- [65] A. Santos, *Phys. Rev. E* **86**, 040102(R) (2012).
- [66] A. Santos, S. B. Yuste, M. López de Haro, G. Odriozola, and V. Ogarko, *Phys. Rev. E* **89**, 040302(R) (2014).
- [67] A. Santos, *A Concise Course on the Theory of Classical Liquids. Basics and Selected Topics*, Lecture Notes in Physics, Vol. 923 (Springer, New York, 2016).
- [68] H. Reiss, H. L. Frisch, and J. L. Lebowitz, *J. Chem. Phys.* **31**, 369 (1959).
- [69] E. Helfand, H. L. Frisch, and J. L. Lebowitz, *J. Chem. Phys.* **34**, 1037 (1961).
- [70] J. L. Lebowitz, E. Helfand, and E. Praestgaard, *J. Chem. Phys.* **43**, 774 (1965).
- [71] A. Santos, M. López de Haro, and S. B. Yuste, *J. Chem. Phys.* **122**, 024514 (2005).
- [72] C. Barrio and J. R. Solana, *Mol. Phys.* **97**, 797 (1999).
- [73] C. Barrio and J. R. Solana, *Phys. Rev. E* **63**, 011201 (2000).
- [74] C. Barrio and J. R. Solana, *Fluid Phase Equil.* **239**, 46 (2006).
- [75] B. D. Lubachevsky and F. H. Stillinger, *J. Stat. Phys.* **60**, 561 (1990).
- [76] V. Ogarko and S. Luding, *J. Chem. Phys.* **136**, 124508 (2012).
- [77] V. Ogarko and S. Luding, *Soft Matter* **9**, 9530 (2013).
- [78] D. Henderson, *Mol. Phys.* **30**, 971 (1975).



- [79] A. Santos, M. López de Haro, and S. B. Yuste, J. Chem. Phys. **103**, 4622 (1995).
- [80] S. Luding, Phys. Rev. E **63**, 042201 (2001).
- [81] S. Luding and O. Strauß, in *Granular Gases*, Lecture Notes in Physics, Vol. 564, edited by T. Pöschel and S. Luding (Springer, Berlin, 2001) pp. 389–409.
- [82] S. Luding and A. Santos, J. Chem. Phys. **121**, 8458 (2004).
- [83] M. López de Haro, S. B. Yuste, and A. Santos, Phys. Rev. E **66**, 031202 (2002).